Journal of Hydrology xxx (2011) xxx–xxx

Contents lists available at SciVerse ScienceDirect

Journal of Hydrology

journal homepage: www.elsevier.com/locate/jhydrol

A model to predict the effects of soil structure on denitrification and N_2O emission

G.M. Laudone [a], G.P. Matthews [a,*], N.R.A. Bird [b], W.R. Whalley [b], L.M. Cardenas [c], A.S. Gregory [b]

[a] Environmental and Fluid Modelling Group, University of Plymouth, Devon PL4 8AA, UK
[b] Department of Sustainable Soils and Grassland Systems, Rothamsted Research, Harpenden, Hertfordshire AL5 2JQ, UK
[c] Department of Sustainable Soils and Grassland Systems, Rothamsted Research, North Wyke, Okehampton, Devon EX20 2SB, UK

ARTICLE INFO

Article history:
Received 15 June 2010
Received in revised form 19 July 2011
Accepted 10 August 2011
Available online xxxx
This manuscript was handled by Philippe Baveye, Editor-in-Chief

Keywords:
Nitrous oxide
Denitrification
Soil structure
Void network model
Anaerobic respiration
Diffusion

SUMMARY

A model of the void space of soil is presented, and used for the *a priori* biophysical simulation of denitrification. The model comprises a single critical percolation channel through a 5 cm stack of four unit cells of a dual-porous void structure. Together, the micro- and macro-porous structures closely replicate the full water retention characteristic of a sandy clay loam soil from the Woburn Experimental Farm operated by Rothamsted Research, UK. Between 1 and 10 micro-porous hot-spot zones of biological activity were positioned at equally spaced distances within 5 cm from the surface, and at either 10 μm or 100 μm from the critical percolation channel. Nitrification and denitrification reactions within the hotspots were assumed to follow Michaelis–Menten kinetics, with estimated values of rate coefficients. Estimates were also made of the threshold values of oxygen concentration below which the anaerobic processes would commence. The pore network was fully saturated following addition of an aqueous 'amendment' of nitrate and glucose which started the reactions, and which mirrored an established laboratory protocol. Diffusion coefficients for Fickian and Crank-Nicolson calculations were taken from the literature, and were corrected for the tortuosity of the micro-porosity. The model was used to show the amount of carbon dioxide, nitrous oxide and molecular nitrogen emerging from the simulated soil with time. Adjustment of the rate coefficient and oxygen threshold concentrations, within the context of a sensitivity analysis, gave emission curves in good agreement with previous experimental measurements. Positioning of the hot-spot zones away from the critical percolation path slowed the increase and decline in emission of the gases. The model and its parameters can now be used for modelling the effect of soil compaction and saturation on the emission of nitrous oxide.

1. Introduction

Denitrification is the anaerobic process by which some species of microbial organisms use nitrate (NO_3^-) as oxidant in the oxidation of organic carbon (C) species. Denitrification is of concern not only because of reduced crop yield though loss of nitrogen (N), but also because one of the gaseous products, nitrous oxide (N_2O), is a greenhouse gas 300 times more potent than carbon dioxide (CO_2), as well as being a cause of stratospheric ozone depletion (Houghton et al., 1991). In agriculture N_2O can be produced from animal manure management systems, inorganic and organic N applied to soils either directly, or indirectly from leached N and from atmospheric deposition. In the UK, the total emission of N_2O from agriculture in 2008 was 81.9 kt N_2O (MacCarthy et al., 2010) comprising 75% of the total UK N_2O emissions. Nitrogen gas (N_2) is also produced in this process, increasing the loss of N from the system, albeit in a benign form.

The transformations undergone by N in soil are complex. The two main processes generating gaseous forms of nitrogen are nitrification and denitrification. These can be represented schematically as shown by the single arrows in Fig. 1. The focus of this work is denitrification, which is controlled by various soil and environmental factors: soil temperature, soil NO_3^- content, C content and quality, soil water status coupled with oxygen (O_2) availability, texture and microbial populations. According to Firestone and Davidson (1989), porosity acts as a distal factor affecting water in soil which also regulates O_2. Aggregate structure and physical disruption are more proximal factors affecting O_2 and C in soil, respectively. Nõmmik (1956) predicted that the size of the pores in soil influence the gas exchange, postulating that poorly aggregated clay soils have small pores that are almost fully water filled at field capacity. Generally clayey soils produce larger N_2O fluxes than sandy soils as they retain more water and may be partially anaerobic due to the smaller textural pores. Additionally, smaller pores provide different micro-sites for bacteria, as inferred from the greater production of N_2O by denitrification in microaggregates (Sey et al., 2008). A well aggregated soil, in contrast, contains large pores that are unsaturated, at least in part, at field capacity and so

* Corresponding author.
E-mail address: pmatthews@plymouth.ac.uk (G.P. Matthews).

0022-1694/$ - see front matter © 2011 Published by Elsevier B.V.
doi:10.1016/j.jhydrol.2011.08.026

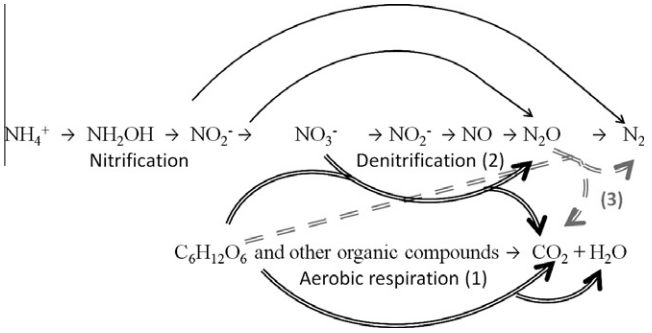

Fig. 1. Nitrification, denitrification and respiration pathways.

gas exchange is facilitated. Oxygen must be limited for denitrification to occur and the threshold O_2 content is dependent on soil water. An experiment on a calcareous clay loamy soil at 29% water saturation showed that partial pressures of O_2 as low as a few kPa can suppress N_2O production (Fazzolari et al., 1998), whereas at 40% water saturation in a mull rendzina soil, N_2O was only produced below an O_2 partial pressure of 4 kPa (Kroeckel and Stolp, 1985). When soils are saturated with water, the supply of O_2 through diffusion is not fast enough to compensate for its consumption by the microorganisms, creating anaerobic conditions that favour denitrification (Khalil et al., 2005), typically peaking at 80% water-filled pore space (Kroeckel and Stolp, 1986; Sey et al., 2008). Nitrous oxide production not only increases markedly with soil moisture, but also with soil compaction (Beare et al., 2009); a future purpose of the current work is to ascertain the extent to which this is a separate effect, or merely because compaction increases the water saturation of the reduced pore space.

Numerous models exist, varying in degree of sophistication, to describe the development of anaerobicity, the reduction of NO_3^- and the production of N_2O and N_2 (Arah and Vinten, 1995; Cho and Mills, 1979; McConnaughey and Bouldin, 1985; Rappoldt and Crawford, 1999; Smith and Macleod, 1980). These models are designed to capture to varying extents the reaction and diffusion of the chemical species involved. Reaction kinetics vary from zero -order through to Michaelis–Menten and competitive Michaelis–Menten kinetics. The models can also allow for detachment of the bacteria from the heterogeneous sites (Clement et al., 1997). The simulation of diffusion in differing soil structures allows for the development and identification of anaerobic zones or microsites in the soil body and for fluxes of gaseous products from the soil surface. However, Heinen (2006) found that most denitrification models could not realistically model the diffusion of the various species involved in the process, especially O_2. Rather they used semi-empirical functions of the soil water content, or water filled pore space, in order to establish whether the anaerobic conditions needed for the denitrification process could be found in the simulated systems.

Clearly of critical importance in any description of denitrification is the presence and location of the microbial biomass responsible for mediating the reduction of NO_3^-. While the simplest and frequently adopted assumption is spatial homogeneity of biomass, there exist reports in the literature relating to localisation and heterogeneity of biomass within the soil pore space (Bundt et al., 2001; Ranjard and Richaume, 2001). A recent review (Morales et al., 2010) suggests that the biologically active micro-porous void space regions of soil, or 'hot-spots', are not located adjacent to the macro-porous structure of the soil. This may seem counterintuitive, because the bacteria would have easier access to nutrients near the macro-porosity. However, they would also be subject to any sudden changes in conditions that may occur. To protect themselves against these potential sudden changes, the active bacteria tend to locate at a buffer distance from the macro-porosity of the soil. Isotopomer studies suggest a complicated distribution of nutrient reservoirs and hotspots (Meijide et al., 2010), such that our postulating of a single distance between the critical percolation path and the hotspots is a major, but useful, approximation.

In this work, we create a model of N_2O emission which builds on the previous studies and additionally incorporates specific structural information at a pore level. Our void structure is based on pore-throat sizes derived from the water retention of a specific soil, as described below. We assume that the microbes are fixed to the surfaces of the microporosity, and that the reagents and products of denitrification and aerobic respiration all diffuse through fully water-filled micro- and macro-porosity. We recognise that this is a major approximation; as observed by Tindall et al. (1995), "the dynamics of NO_3^- transport and transformation in unsaturated soils are affected by small, localised variations in the soil moisture content profile, the gaseous diffusion coefficient of the soil, the rate at which the NO_3^- pulse passes through the soil, the solubility of N_2O and N_2 and the diffusion of the gases through the soil solution, and the development of a water content profile in the soil". More specifically, we model an established laboratory system in which (i) the soil is initially flushed with He and O_2 (4:1 by volume) initially to remove N_2, and then to carry the gaseous products from denitrification to a gas chromatograph, (ii) the water content of the sample is initially adjusted such that an "amendment" of NO_3^- and glucose just brings it to full saturation (Cardenas et al., 2003), and (iii) in which the NO_3^- and glucose concentrations in the amendment cause the denitrification to be NO_3^--limiting but not glucose limiting within the 2 week time-scale of the experiment. We investigate the influence of the spatial disposition of the biological hot-spots by modelling the diffusion of O_2, C and NO_3^- to, and denitrification products from, these biologically active locations.

2. Modelling

The construction of the biophysical model is in three stages. Firstly, macro- and micro-porous unit cells are generated which, when assembled together, precisely match the full retention characteristics of the chosen soil. Secondly, these unit cells are used as the building blocks of a larger scale simplified structure with overall dimensions more appropriate to the experimental samples we are simulating. Thirdly, within this larger scale structure, the biological activity must be sited and the diffusion of nutrients and gases calculated. These three stages are described in the following three sections.

2.1. The pore-network model

The network model Pore-Cor has been previously used to simulate and comprehend the effect on soil structure and hydraulic conductivity of soil texture (Johnson et al., 2003), clover roots (Holtham et al., 2007) and compaction (Matthews et al., 2010). The void structure of a porous medium is represented as a series of unit cells. Each unit cell is made of an array of 1000 nodes equally spaced in a Cartesian cubic-close-packed array. Cubic pores are positioned with their centres at each node, and are connected by other, smaller cylindrical pores (termed throats) in each Cartesian direction. The unit cells have periodic boundary conditions – i.e. each connects to a replicate in every Cartesian direction. Fluids can move out of one unit cell into the opposite face of the replicate, and so also appear in the original unit cell, thus conserving mass, as described in more detail below. The throat size distributions follow an Euler beta function (Price et al., 2009), which can include Gauss-

Please cite this article in press as: Laudone, G.M., et al. A model to predict the effects of soil structure on denitrification and N_2O emission. J. Hydrol. (2011), doi:10.1016/j.jhydrol.2011.08.026

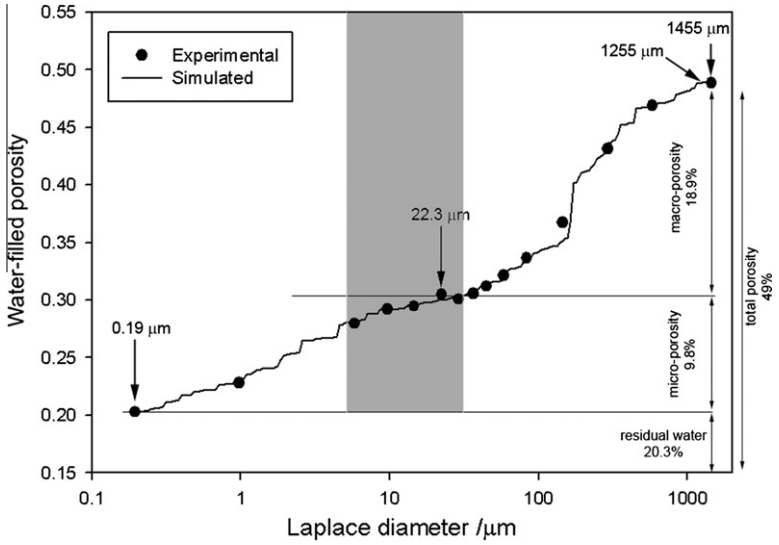

Fig. 2. Conversion of the water retention characteristic using the Laplace Eq. (1), showing porosities, and the field capacity region shown shaded.

ian-like, Poisson-like and bimodal distributions, and the pores are sized proportionally to the largest throat entering them.

The void network structure for the present work derives from the inverse modelling of the water retention curve of a 4 mm-sieved and repacked soil sample taken from Warren field at the Woburn Experimental Farm in Bedfordshire, UK, operated by Rothamsted Research. The water retention measurements were converted to water-filled porosity by multiplying the gravimetric water content of the sample by its dry bulk density. The sizes of the void features were calculated from the Laplace equation, which gives the diameter d of a cylinder which can be intruded by a non-wetting fluid (air displacing water) at an applied differential pressure P:

$$d = \frac{4\gamma \cos\theta}{P} \quad (1)$$

It was assumed that the interfacial tension γ of water in soil is 0.075 N m^{-1} and that water is fully wetting, so that the contact angle at the interface $\theta = 0°$. The water retention curve, expressed in this way, is shown on Fig 2. The percolation curve has an obvious step around 200 μm, with a slightly flatter region around 10–30 μm. Therefore it is not unrealistic to view it as bimodal, implying a region of macro-pores with Laplace diameters up to 1455 μm, and a region of micro-pores with diameters as small as 0.19 μm. A Laplace diameter of 22.3 μm correlates with a tension of around -14 kPa that is in the 'field capacity' range from −5 to −33 kPa (shaded grey) – i.e. it is a size above which pores tend to drain by gravity, and below which the plants can begin to extract "available" water (Richards and Weaver, 1944). So the choice of 22.3 μm as the threshold between microporosity and macroporosity is sensible with respect to the behaviour of water in soil, as well as with respect to the shape of the water retention curve. The overall porosity of the Warren soil sample was 49.0%. The porosity fully described by the water retention curve was 28.7%, split between 18.9% macro-porosity and 9.8% micro-porosity, Fig. 2.

A Boltzmann-annealed amoeboid simplex was used to generate two void networks, corresponding to the water retention characteristics above and below -14 kPa. For mathematical simplicity, the hot-spots within the soil were assumed to be clustered into individual zones which filled cubic regions of side length 100 μm, although in reality they would be much more widely and diversely spread. Fig. 3a shows the dual porous void structure, which has an almost identical water retention characteristic at all tensions to that shown in Fig. 2. The dendritic critical percolation path, i.e. where air first breaks through the structure as water is removed at increasing tensions, is shown in plain light grey. A micro-porous hot-spot zone, shown speckled grey or yellow and blue, in this case adjacent to the critical percolation path, is marked in Fig 3a and zoomed into through Fig 3b–d. In Fig. 3a and c, the xz planes at $y = 0$, and yz planes at $x = 0$ are standard periodic boundaries in both the macro- and micro-structure – i.e. all fluid passes through the boundary, normal to the plane, and enters the connected replicate unit cell. By contrast, the xy planes at $z = l_{\text{macrocell}}$ or $z = l_{\text{micro-cell}}$ act as super-sources of fluid, and the xy planes at $z = 0$ act as a super-sinks.

2.2. Larger scale simplified model

The size of the unit cell shown in Fig. 3a is 13.81 mm. This is adequate to describe the fluid dynamics within the modelled soil samples; however, the bio-chemical phenomena of aerobic respiration and denitrification occur deeper into the soil over depths of the order of centimetres. In order to resolve this issue it is not possible to stack up several dual-porous cells, as this would lead to an unrealistic repetition of the dendritic percolation paths in the vertical direction, and it would also cause boundary condition problems where the top and bottom of these tree-like macro-porous paths join. As a consequence, we decided to present a simplified soil model, where the macro-porous volume is approximated to a 5 cm vertical tube, with the micro-porosity adjacent to it (Fig. 4). The structure shown in the figure then represents a soil surface area of 13.81 mm × 13.81 mm, i.e. 1.91 cm^2. The simplified model can be justified by realising that the diffusion through the tortuous macro-porous path is orders of magnitude faster than the diffusion through the micro-porous structure, and thus neglecting the tortuosity of the macro-porous structure would cause a negligible error. The 0.3 mm diameter of the vertical tube is chosen as the size corresponding to the breakthrough pressure of the simulated macro-porous cell, so it is exactly equivalent to a non-tortuous percolation path through the stack of approximately four unit cells shown in the figure. Hot spot zones fill 100 μm cubes, positioned either 10 μm or 100 μm from the critical percolation path as shown in Fig. 4. The pore structure of the microporous zone is that of Fig. 3. However only two properties of the micro-structure are used, namely the tortuosity and the micro-porosity, as described below.

Please cite this article in press as: Laudone, G.M., et al. A model to predict the effects of soil structure on denitrification and N_2O emission. J. Hydrol. (2011), doi:10.1016/j.jhydrol.2011.08.026

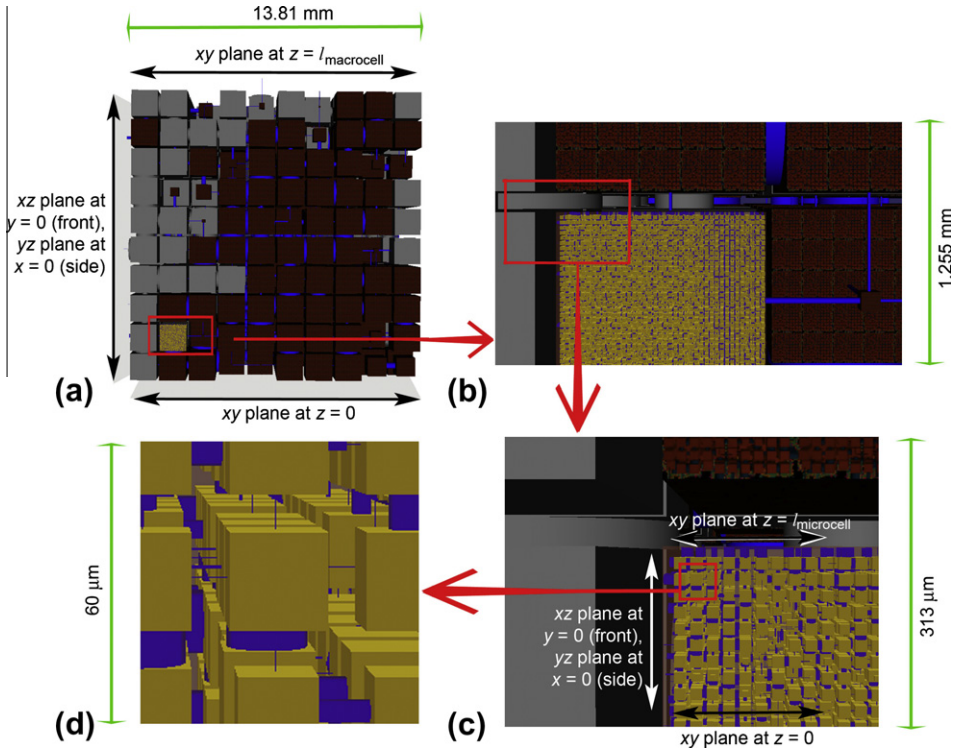

Fig. 3. Dual porous structure of soil.

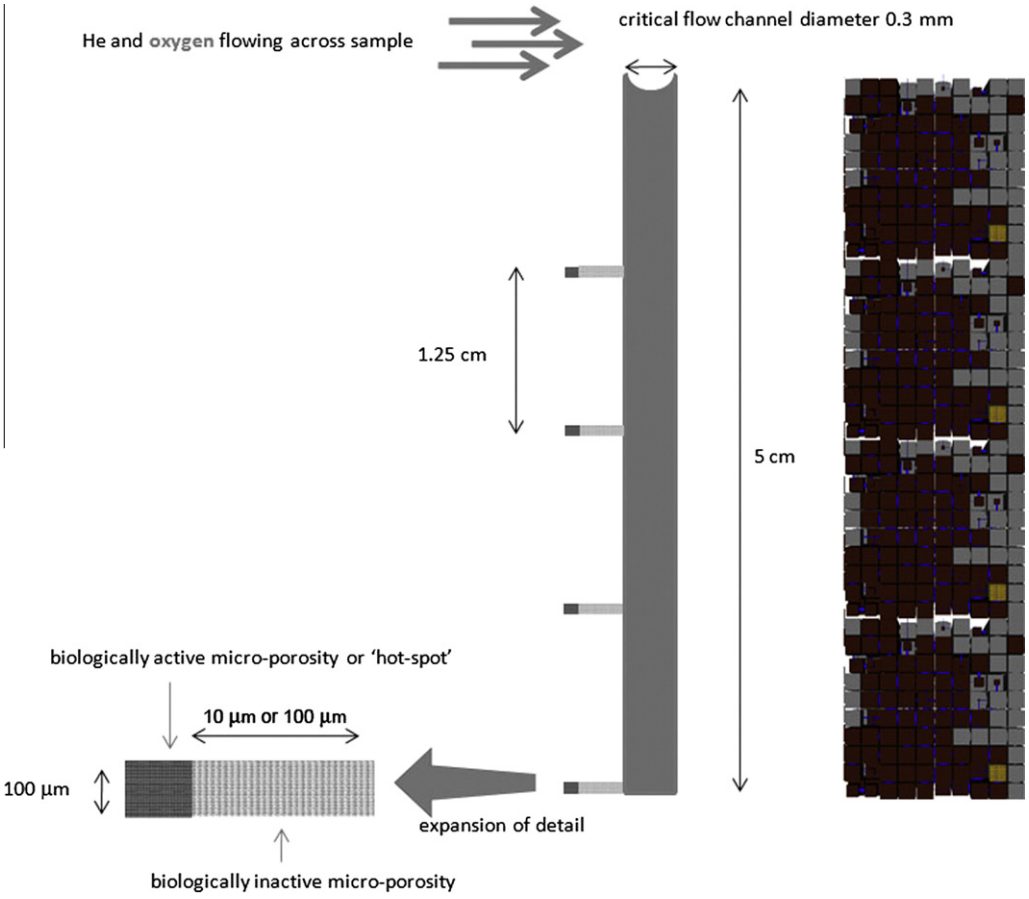

Fig. 4. Schematic representation of the system modelled in this work, and the corresponding dual-porous network model, shown on the right. The features have the dimensions shown; they are not drawn to scale. The hotspots are equally spaced down the 5 cm length of the critical flow channel – the arrangement shown is for 4 hot-spots.

Please cite this article in press as: Laudone, G.M., et al. A model to predict the effects of soil structure on denitrification and N_2O emission. J. Hydrol. (2011), doi:10.1016/j.jhydrol.2011.08.026

Table 1
Values of the bio-chemical modelling parameters. 1 = Weast and Astle (1979), E = estimated.

Parameter	Value	Units	Source
Initial labile carbon concentration in hot-spots	1.0×10^{-1}	mol dm^{-3}	E
V_{max} aerobic respiration	1.20×10^{2}	mol dm^{-3} s^{-1}	E
K_m Michaelis–Menten constant aerobic respiration	1.40×10^{-4}	mol dm^{-3}	E
V_{max} production N_2O	1.20	mol dm^{-3} s^{-1}	E
K_m Michaelis–Menten constant N_2O production	1.40×10^{-4}	mol dm^{-3}	E
V_{max} N_2 production	1.20	mol dm^{-3} s^{-1}	E
K_m Michaelis–Menten constant N_2 production	1.40×10^{-4}	mol dm^{-3}	E
[O_2] threshold for N_2O production	1.0×10^{-4}	mol dm^{-3}	E
[O_2] threshold for N_2 production	7.8×10^{-6}	mol dm^{-3}	E
D_{aq} O_2	$1.97e^{-9}$	m^2 s^{-1}	1
D_{aq} N_2	1.90×10^{-9}	m^2 s^{-1}	1
D_{aq} N_2O	$1.80e^{-9}$	m^2 s^{-1}	1
D_{aq} CO_2	1.96×10^{-9}	m^2 s^{-1}	1
D_{aq} glucose	6.00×10^{-10}	m^2 s^{-1}	1
D_{aq} nitrate	1.70×10^{-9}	m^2 s^{-1}	1
D_{air} N_2	2.00×10^{-5}	m^2 s^{-1}	1
D_{air} N_2O	1.43×10^{-5}	m^2 s^{-1}	1
D_{air} CO_2	1.60×10^{-5}	m^2 s^{-1}	1

2.3. Reaction and diffusion calculations

In this work we assume that the gas flushing time before the amendment is long enough to ensure that the concentration of gas species has reached a Henry's law equilibrium:

$$k_H = c_{aq}/p_{gas} \tag{2}$$

where k_H is Henry's constant, given by the ratio between the concentration of the species in the aqueous phase and the partial pressure of the species in the gas phase. The effect of temperature is also taken into account and the Henry's constant for each species is corrected according to:

$$k_{H1} = k_{H2} \exp\left[\frac{\Delta H_{sol}}{R}\left(\frac{1}{T_1} - \frac{1}{T_2}\right)\right] \tag{3}$$

where k_{H1} and k_{H2} are the values of Henry's constant at the experimental temperature T_1 and at T_2 = 298.15 K respectively and ΔH_{sol} is the enthalpy of solution (Sander, 1999).

The network porosity and tortuosity of the micro-porous unit cell are used for the calculation of a corrected diffusion coefficient which takes into account the effect of network porosity and tortuosity, according to the relation:

$$D_{corr} = \frac{D\phi}{\tau^2}, \tag{4}$$

where D_{corr} is the corrected diffusion coefficient, D is the molecular diffusion coefficient, τ is the tortuosity of the simulated soil micro-porosity and ϕ is the soil micro-porosity. The tortuosity is the median path length of successive three-dimensional random walks through the sample, with path probabilities weighted according to the cross-sectional areas of individual features (Spearing and Matthews, 1991).

The bio-chemical activity is assumed to be concentrated in hot-spots zones. These zones are of micro-porous void volume, equally distributed along the length of the macro-porous path as shown, for the case of four hot-spot zones, in Fig. 4. In the void volume of the hot-spot zones, the nitrification/denitrification/respiration reactions are simplified to three overall reactions, as shown by the double-lined arrows in Fig. 1:

(1) Aerobic respiration, which converts glucose and O_2 to CO_2 and H_2O.
(2) Conversion of glucose and NO_3^- to N_2O and CO_2.
(3) Conversion of N_2O to N_2.

The reactions were all assumed to follow Michaelis–Menten kinetics, which involves initial equilibrium with an unspecified intermediate. In practice, the initial equilibrium always proved to be far over towards the intermediate species, and so the resulting kinetics for the reactions were all simply first order. The production of N_2O and the production of N_2 were triggered by the O_2 concentration in each hot-spot. The concentration of O_2 needed for reaction (2) to start was higher than that required to trigger reaction (3). Neither of the values of these threshold O_2 concentrations is known, so different values have been used in the simulations to test the sensitivity of the model, Table 1.

The various chemical species in the system (glucose, NO_3^-, N_2O, N_2, O_2 and CO_2) can diffuse in or out of a hot-spot according to the concentration gradients between the hot-spot and the horizontally neighbouring layer of the critical percolation path. As this diffusion process takes place within the micro-porosity of the soil, the free molecular diffusion coefficients of the species were corrected to take into account the porosity and the tortuosity of the micro-porous unit cell, calculated as described above. Fickian diffusion equations were used to describe the diffusion in and out of the hot-spot zones.

The diffusion of the species along the water filled macro-porous path was modelled with a Crank-Nicolson method (Pandey et al., 1982), for which the critical flow channel is split into 500 layers of height 100 μm. The diffusion into the He/O_2 flushing stream was calculated using a mass transfer coefficient (Tosun, 2002):

$$M = (Sh \cdot D_{air})/L \tag{5}$$

where M is the mass transfer coefficient, Sh is the Sherwood number, D_{air} is the diffusion coefficient in air and L is the side length of the surface of top layer of the critical percolation path top layer exposed to the gas flow.

$$Sh = 0.332 Re^{1/2} Sc^{1/3} \tag{6}$$

where Re is the Reynolds number and Sc is the Schmidt number $Sc = \nu D_{air}$, ν being the kinetic viscosity of air.

The values used in the simulations are presented in Table 1. Aerobic respiration, denitrification and gas diffusion and emission from the simplified soil geometry were simulated initially for increasing number of active hot-spot zones and for two different values of distance between the hot-spot zones and the critical percolation path, namely 10 μm and 100 μm. The influence of the parameters in Table 1 on the model results was also investigated, as presented in the Sensitivity Analysis section.

Please cite this article in press as: Laudone, G.M., et al. A model to predict the effects of soil structure on denitrification and N_2O emission. J. Hydrol. (2011), doi:10.1016/j.jhydrol.2011.08.026

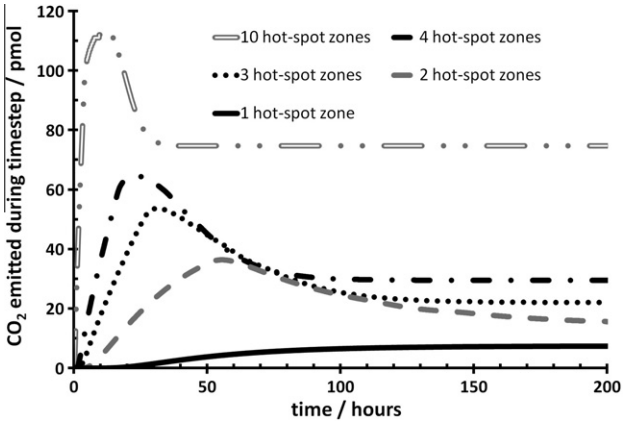

Fig. 5. CO_2 emission from simulated soil structures with 1–10 hot-spots located at 10 μm from the macro-porous path. The timestep is 0.1 s in all the simulations.

3. Results and discussion

This work focuses on the emission of N_2 and N_2O; hence, only one representative graph of the results of CO_2 emission is shown, Fig. 5. (Note that the axis scales of all the graphs vary.) The CO_2 emissions reach a steady-state condition. The simulations are carried out for about 350 h (14.6 days), which is not long enough for the system to use up all the glucose. If the simulations were allowed to run for a longer time, these curves would show a drop of CO_2 emission as the system ran out of glucose.

The units of the simulated gaseous emissions are very small, with units of fmols (10^{-15} mols) or pmoles (10^{-12} moles). This is due to the small size of the simulation, which corresponds to only one 300 μm wide macro-porous channel and its associated micro-porosity, situated within a stack of cubic macro-porous cells with a side-length of 13.81 mm. The surface area represented is 1.91 cm^2, as detailed above. The model also uses a short timestep of 0.1 s. Simple linear upscaling of the model shows that 1.0 pmol emitted during one 0.1 s timestep corresponds to 1.26 kg ha^{-1} day^{-1} or 1.99 kg ha^{-1} day^{-1} of N_2 and N_2O respectively. These emissions are in the same range as those observed experimentally by Cardenas et al. (2003) which are of order of magnitude of 10^{-1}–10^2 kg ha^{-1} day^{-1}, depending on experimental conditions.

When the hot-spot zones of biological activity were placed 10 μm away from the critical percolation path, the simulation gave the results shown in Figs. 6a and b. Fig. 6a shows that the peak value of N_2O production increased with increasing number of hot-spot zones; however the areas under the curves, representing the cumulative production during the simulation time were very similar (140–150 pmol), with the exception of the case of the system with 1 hot-spot only (0.11 fmol). An increasing number of hot-spot zones causes the N_2O emission to happen faster, for a shorter amount of time. However the effect on total (rather than peak) emissions of increasing the number of hot-spot zones above 2 is negligible. The zones are equally spaced over the same depth profile. So increasing their number makes the depth interval between the zones smaller, and increases the number of zones which are closer to the top of the surface which are less able to reach the anaerobic conditions necessary for denitrification to occur.

Fig. 6b shows the extent of simulated N_2 emission. The simulations run with the initial estimated value of modelling parameters shown in Table 1 yielded total (rather than peak) N_2 emissions four orders of magnitude larger than total N_2O emissions shown in Fig. 6a. The N_2 emission curves reached steady-state conditions, with most of the N_2O produced in the hot-spot zones being converted into N_2. These steady-state conditions would carry on until the nutrients in the system were exhausted, which does not happen within the duration of the simulations. The N_2 emission curves reached their peaks 20–40 h later than the N_2O emission curves, a phenomenon often observed in experimental results on soil denitrification.

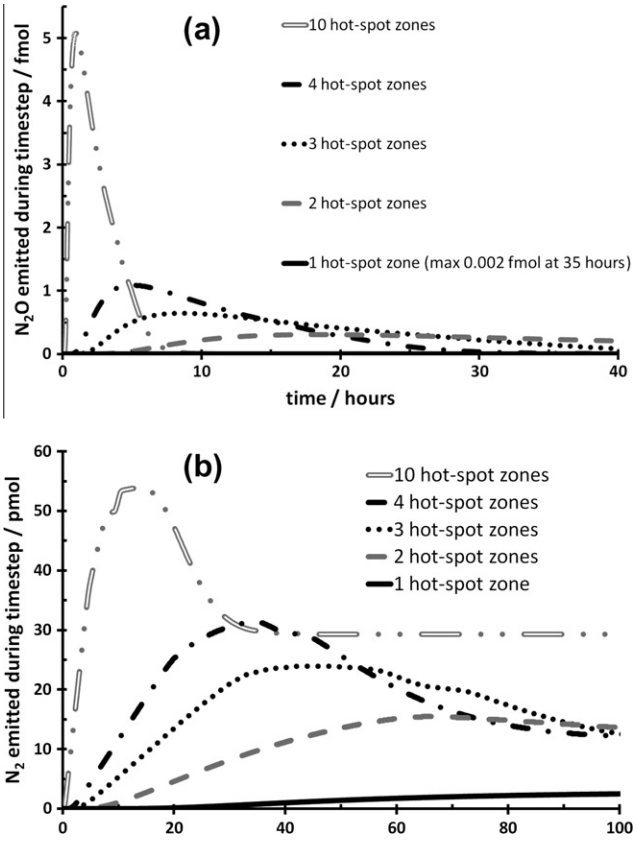

Fig. 6. (a) N_2O and (b) N_2 emissions from simulated soil structures with 1–10 hot-spots located at 10 μm from the macro-porous path. The N_2O emission from 1 hot-spot is on the baseline.

Identical simulations were then carried out, except that the hot-spot zones were at a distance of 100 μm rather than 10 μm from the critical percolation path. Fig. 7a and b show the results of N_2O and N_2 emissions respectively. It can be seen that the simulations gave similar trends to those showed previously for hot-spot zones closer to the critical percolation path. However, the upwards and downwards slopes in the curves shown in Fig. 7a and b are very slightly less steep for N_2, and much less steep (noting the change of time axis) for N_2O than the slopes of the corresponding curves in Fig. 6a and b, showing the effect of diffusion of chemical species over a longer length of biologically inactive micro-porosity. Despite the fact that hot-spot zones further away from the critical percolation path would reach the anaerobic conditions required for denitrification in a shorter amount of time, the products of the denitrification reactions take longer to migrate from the hot-spot zones to the critical percolation path and to reach the surface of the system.

4. Sensitivity analysis

The precise kinetics of the simulated reactions depend on the microbial populations and the microstructure of soil substrate. These have not been experimentally measured, so values of rate coefficients and concentration thresholds have been estimated. To discover the importance of the accuracy of these estimates to the final results, the estimated reaction rates and thresholds were subjected to a sensitivity analysis, as follows.

Please cite this article in press as: Laudone, G.M., et al. A model to predict the effects of soil structure on denitrification and N_2O emission. J. Hydrol. (2011), doi:10.1016/j.jhydrol.2011.08.026

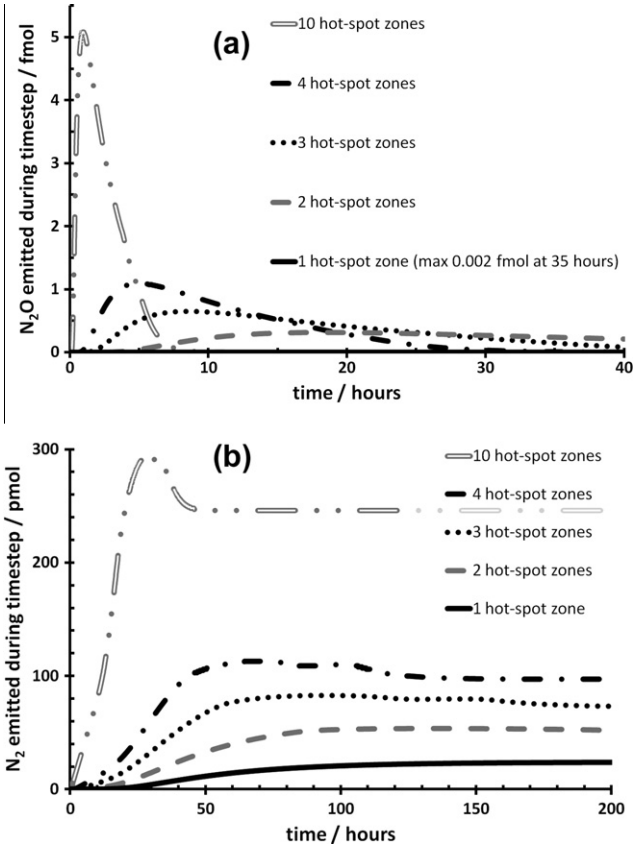

Fig. 7. (a) N_2O and (b) N_2 emissions from simulated soil structures with 1–10 hot-spots located at 100 μm from the macro-porous path. The N_2O emission from 1 hot-spot is on the baseline.

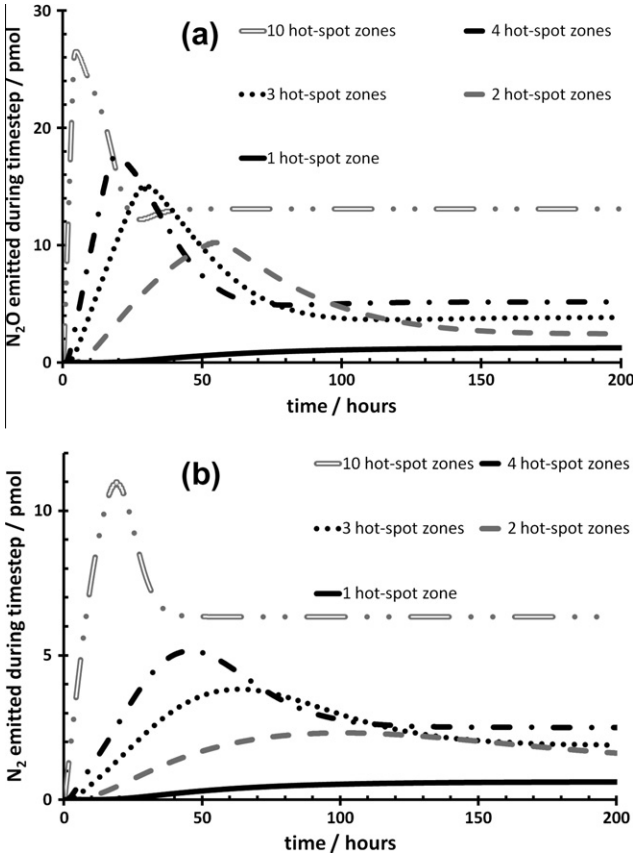

Fig. 8. (a) N_2O and (b) N_2 emissions at lower value of maximum rate for reaction producing N_2. The simulated soil structures have 1–10 hot-spot zones located at 10 μm from the macro-porous path.

4.1. Effect of the reaction rate of N_2 production

As observed in Figs. 6 and 7, the initial set of modelling parameters resulted in very large N_2 to N_2O emission ratios. However, from the work of Cardenas et al. (2003) it appears that the ratio of N_2:N_2O emission is in the range 1:1 to 1:3. In order to obtain results closer to those shown in experimental work by Cardenas et al. the maximum reaction rate coefficient of the N_2 producing reaction was decreased by a factor 10, while all other parameters were kept constant. Fig. 8a and b shows the resulting N_2O and N_2 emission curves respectively. The change in maximum rate coefficient caused the N_2O emission to increase by 3–4 orders of magnitude, whereas the emission of N_2 decreased by a factor of around 3. The slower conversion of N_2O to N_2 allowed more N_2O to diffuse out of the hot-spot zones and reach the surface of the system. These sets of simulations gave ratios of N_2 to N_2O production of the same order of magnitude, as observed experimentally.

Comparing Fig. 6a and b with Fig. 8a and b it can also be observed that both N_2 and N_2O emissions peaked a few hours later when a lower maximum reaction rate coefficient was used in the simulations. The time-lag between the N_2 and N_2O emission peaks was also slightly increased by this perturbation.

4.2. Effect of the values of O_2 thresholds

The O_2 threshold concentrations needed in the hot-spot zones to initiate the conversion of NO_3^- to N_2O and of N_2O to N_2 had been initially estimated as 1.0×10^{-4} and 7.8×10^{-6} mol dm^{-3} respectively. In order to investigate the sensitivity of the model to these parameters, their value was reduced by one order of magnitude while all other parameters were kept the same as in the previous section. The resulting N_2O emission peaks were between 1% and 6% higher, at times between 1% less and 21% longer than those shown in Fig. 7. The N_2 emission peaks were between 7% and 13% lower, at times within 2% of those shown in Fig 7. The lack of sensitivity to the O_2 threshold suggests that the reaction rate of aerobic respiration is fast enough to reach the anaerobic conditions needed to initiate the denitrification process, despite the reduction in the O_2 threshold values.

Finally, the hot-spot O_2 required to initiate the conversion of N_2O to N_2 was reduced by one more order of magnitude, increasing the difference in O_2 conditions needed for the two denitrification reactions to occur. This had a greater effect, with the N_2O emission peaks increasing by between 6% and 13% relative to that shown in Fig 7, at times between 2% less and 20% greater, while N_2 peaks showed a reduction of 17–26%. Because of the lower O_2 threshold needed to initiate the conversion of N_2O to N_2, a larger amount of N_2O produced in the hot-spot zones could leave the biologically active sites and reach the top surface of the system before the conditions in the hot-spot zones allowed for its conversion to N_2.

5. Summary and conclusions

A novel model for the simulation of denitrification and N_2O emission has been presented, featuring precise and explicit positional relationships between macro- and micro-porosity. The biochemical activity of aerobic respiration and denitrification was assumed to be taking place in active regions, or hot-spot zones, of the micro-porous void volume, while the transport of the chemical species produced in the hot-spot zones was assumed to be taking

Please cite this article in press as: Laudone, G.M., et al. A model to predict the effects of soil structure on denitrification and N_2O emission. J. Hydrol. (2011), doi:10.1016/j.jhydrol.2011.08.026

place along the macro-porous critical percolation path of a simulated soil network structure.

The effect of various parameters of the model on the gaseous emission was investigated. It was observed that the distance of the hot-spot zones of bio-chemical activity from the macro-porous path plays a role, influencing the diffusion of chemical species into and out of the hot-spot zones. The slower response of the system to an amendment of NO_3^- and glucose when this hot-spot distance was increased is in accord with the considerations of Morales et al. (2010).

It was also shown how hot-spot zones located too close to the top surface of the system will contribute less to the denitrification process as they will receive O_2 more readily from the top surface of the system and they will struggle to reach the anaerobic conditions needed to initiate the production of N_2O and N_2. In the present model, the bacterial populations are static, but in the field it is likely that bacterial populations will flourish in optimum positions within the soil matrix.

The effects of the value of O_2 in the hot-spot zones required to start the conversion of N_2O to N_2 and of the reaction rate of the conversion of N_2O to N_2 were also investigated. It was observed that it is possible to delay the production and emission of N_2 and to change the ratio of N_2O to N_2 emission by changing the value of these parameters.

The importance of the mathematical experiments presented in this work is that they give orders of magnitude for parameters which are experimentally elusive and which therefore have never been measured. Indeed, it is difficult to envisage how, for example, the *in vivo* O_2 threshold concentrations for nitrification and denitrification could be measured within hotspots without perturbing either the micro-porosity or the bacterial populations.

Most concern in the literature is with respect to the effect of saturation and compaction on the production of N_2O, for example the work of Ball et al. (2008). Now the fundamental bio-physical parameters have been determined, these simulations will be carried out to determine whether soil structure, or simply saturation, is the determining factor when the biological parameters are constrained.

Acknowledgements

This work was funded by the UK Biotechnology and Biological Sciences Research Council (BBSRC) programme for Understanding Soil Quality and Resilience [Grant Numbers BB/E001793 and BB/E001580]. Rothamsted Research is an institute of the BBSRC.

References

Arah, J.R.M., Vinten, A.J.A., 1995. Simplified models of anoxia and denitrification in aggregated and simple-structured soils. Eur. J. Soil Sci. 46 (4), 507–517.

Ball, B.C., Crichton, I., Horgan, G.W., 2008. Dynamics of upward and downward N_2O and CO_2 fluxes in ploughed or no-tilled soils in relation to water-filled pore space, compaction and crop presence. Soil Tillage Res. 101 (1–2), 20–30.

Beare, M.H., Gregorich, E.G., St-Georges, P., 2009. Compaction effects on CO_2 and N_2O production during drying and rewetting of soil. Soil Biol. Biochem. 41 (3), 611–621.

Bundt, M., Widmer, F., Pesaro, M., Zeyer, J., Blaser, P., 2001. Preferential flow paths: biological 'hot spots' in soils. Soil Biol. Biochem. 33 (6), 729–738.

Cardenas, L.M., Hawkins, J.M.B., Chadwick, D., Scholefield, D., 2003. Biogenic gas emissions from soils measured using a new automated laboratory incubation system. Soil Biol. Biochem. 35 (6), 867–870.

Cho, C.M., Mills, J.G., 1979. Kinetic formulation of the denitrification process in soil. Can. J. Soil Sci. 59 (3), 249–257.

Clement, T.P., Peyton, B.M., Skeen, R.S., Jennings, D.A., Petersen, J.N., 1997. Microbial growth and transport in porous media under denitrification conditions: experiments and simulations. J. Contam. Hydrol. 24 (3–4), 269–285.

Fazzolari, E., Guerif, J., Nicolardot, B., Germon, J.C., 1998. A method for the preparation of repacked soil cores with homogeneous aggregates for studying microbial nitrogen transformations under highly controlled physical conditions. Eur. J. Soil Biol. 34 (1), 39–45.

Firestone, M.K., Davidson, E.A., 1989. Microbiological basis of NO and N_2O production and consumption in soil. In: Andreae, M.O., Schimel, D.S. (Eds.), Exchange of Trace Gases between Terrestrial Ecosystems and the Atmosphere. Life Sciences Research Report, pp. 7–21.

Heinen, M., 2006. Simplified denitrification models: overview and properties. Geoderma 133, 444–463.

Holtham, D.A.L., Matthews, G.P., Scholefield, D.S., 2007. Measurement and simulation of the void structure and hydraulic changes caused by root-induced soil structuring under white clover compared to ryegrass. Geoderma 142, 142–151.

Houghton, J.T., Jenkins, G.J., Ephraums, J.J., 1991. Climate Change. The IPCC Scientific Assessment. Cambridge University Press, Cambridge.

Johnson, A., Roy, I.M., Matthews, G.P., Patel, D., 2003. An improved simulation of void structure, water retention and hydraulic conductivity in soil, using the Pore-Cor three-dimensional network. Eur. J. Soil Sci. 54 (3), 477–489.

Khalil, K., Renault, P., Mary, B., 2005. Effects of transient anaerobic conditions in the presence of acetylene on subsequent aerobic respiration and N_2O emission by soil aggregates. Soil Biol. Biochem. 37 (7), 1333–1342.

Kroeckel, L., Stolp, H., 1985. Influence of oxygen on denitrification and aerobic respiration in soil. Biol. Fertil. Soils 1 (4), 189–193.

Kroeckel, L., Stolp, H., 1986. Influence of the water regime on denitrification and aerobic respiration in soil. Biol. Fertil. Soils 2 (1), 15–21.

MacCarthy, J. et al., 2010. UK Greenhouse Gas Inventory, 1990 to 2008 Annual Report for Submission under the Framework Convention on Climate Change. AEAT/ENV/R/2978.

Matthews, G.P. et al., 2010. Measurement and simulation of the effect of compaction on the pore structure and saturated hydraulic conductivity of grassland and arable soil. Water Resour. Res. 46 (5), W05501.

McConnaughey, P.K., Bouldin, D.R., 1985. Transient microsite models of denitrification: I. Model development. Soil Sci. Soc. Am. J. 49, 886–891.

Meijide, A. et al., 2010. Dual isotope and isotopomer fractionation for the understanding of N_2O production and consumption during denitrification in an arable soil. Eur. J. Soil Sci. 61 (3), 364–374.

Morales, V.L., Parlange, J.Y., Steenhuis, T.S., 2010. Are preferential flow paths perpetuated by microbial activity in the soil matrix? A review. J. Hydrol. 393 (1–2), 29–36.

Nõmmik, F., 1956. Investigations on denitrification in soil. Acta Agric. Scand. 13, 34.

Pandey, R.S., Singh, S.R., Sinha, B.K., 1982. An extrapolated Crank–Nicolson method for solving the convection–dispersion equation with non-linear adsorption. J. Hydrol. 56, 277–285.

Price, J.C., Matthews, G.P., Quinlan, K., Sexton, J., Matthews, A.G.D., 2009. A depth filtration model of straining within the void networks of stainless steel filters. AIChE J. 55 (12), 3134–3144.

Ranjard, L., Richaume, A.S., 2001. Quantitative and qualitative microscale distribution of bacteria in soil. Res. Microbiol. 152 (8), 707–716.

Rappoldt, C., Crawford, J.W., 1999. The distribution of anoxic volume in a fractal model of soil. Geoderma 88 (3–4), 329–347.

Richards, L.A., Weaver, L.R., 1944. Moisture retention by some irrigated soils as related to soil moisture tension. J. Agric. Res. 69, 215–235.

Sander, R., 1999. Compilation of Henry's Law Constants for Inorganic and Organic Species of Potential Importance in Environmental Chemistry.

Sey, B.K., Manceur, A.M., Whalen, J.K., Gregorich, E.G., Rochette, P., 2008. Small-scale heterogeneity in carbon dioxide, nitrous oxide and methane production from aggregates of a cultivated sandy-loam soil. Soil Biol. Biochem. 40 (9), 2468–2473.

Smith, O.B., Macleod, G.K., 1980. Digestibility of wet cage layer excreta and an excreta-supplemented diet by cattle as determined by 2 methods. Animal Feed Sci. Technol. 5 (1), 77–85.

Spearing, M.C., Matthews, G.P., 1991. Modelling characteristic properties of sandstones. Trans. Por. Med. 6, 71–90.

Tindall, J.A., Petrusak, R.L., McMahon, P.B., 1995. Nitrate transport and transformation processes in unsaturated porous-media. J. Hydrol. 169 (1–4), 51–94.

Tosun, I., 2002. Modelling in Transport Phenomena: A Conceptual Approach. Elsevier, Amsterdam.

Weast, R.C., Astle, M.J., 1979. CRC Handbook of Chemistry and Physics, 60. CRC Press, Inc., Florida, USA.

Please cite this article in press as: Laudone, G.M., et al. A model to predict the effects of soil structure on denitrification and N_2O emission. J. Hydrol. (2011), doi:10.1016/j.jhydrol.2011.08.026